Applied Thermal Engineering 50 (2013) 429–436

Contents lists available at SciVerse ScienceDirect

Applied Thermal Engineering

journal homepage: www.elsevier.com/locate/apthermeng

Analytical analysis of heat transfer and pumping power of laminar nanofluid developing flow in microchannels

Manu Mital*

Mechanical and Nuclear Engineering, Virginia Commonwealth University, Engineering East Hall, Room E3232, 401 West Main Street, Virginia Com., Richmond, VA 23284, United States

HIGHLIGHTS

- ► Validated model is used to investigate heat transfer and pumping power in nanofluids.
- ► Particles improve heat transfer but increased pumping power partially offsets the gains.
- ► Ratio of heat transfer coefficient of nanofluid over pure fluid at same pumping power is denoted HTR.
- ► HTR significantly depends on particle size and volume fraction; weakly on Reynolds number.
- ► For any given Reynolds number, HTR is maximized using smallest particle size and determining an optimum volume fraction.

ARTICLE INFO

Article history:
Received 11 February 2012
Accepted 8 July 2012
Available online 14 August 2012

Keywords:
Nanofluids
Nanoparticles
Microchannels
Developing laminar flow

ABSTRACT

Thermal management issues are limiting barriers to high density electronics packaging and miniaturization. Liquid cooling using micro and mini channels is an attractive alternative to large and bulky aluminum or copper heat sinks. These channels can be integrated directly into a chip or a heat spreader, and cooling can be further enhanced using nanofluids (liquid solutions with dispersed nanometer-sized particles) due to their enhanced heat transfer effects reported in literature. The goals of this study are to evaluate heat transfer improvement of a nanofluid heat sink with developing laminar flow forced convection, taking into account the pumping power penalty. The phrase heat transfer enhancement ratio (HTR) is used to denote the ratio of average heat transfer coefficient of nanofluid to water at the same pumping power. The proposed model uses semi-empirical correlations to calculate nanofluid thermophysical properties. The predictions of the model are found to be in good agreement with experimental studies. The validated model is used to identify important design variables (Reynolds number, volume fraction and particle size) related to thermal and flow characteristics of the microchannel heat sink with nanofluids. Statistical analysis of the model showed that the volume fraction is the most significant factor impacting the HTR, followed by the particle diameter. The impact of the Reynolds number and other interaction terms is relatively weak. The HTR is maximized at smallest possible particle diameter (since smaller particles improve heat transfer but do not impact pumping power). Then, for a given Reynolds number, an optimal value of volume fraction can be obtained to maximize HTR. The overall aim is to present results that would be useful for understanding and optimal design of microchannel heat sinks with nanofluid flow.

1. Background and introduction

Power and semiconductor electronic systems find widespread application in residential, commercial, military and space environments. In everyday life, these systems are commonly used in televisions, automobiles, telephones, computers, etc. Due to their widespread use, electronics chips need to operate reliably under a wide variety of environmental conditions. One of the key factors that affect reliability is thermal management. The difference between the input and the output energy in an electronic system is converted to heat, which must be removed efficiently to prevent overheating and chip failures. Efficient thermal management still remains a challenge that needs to be addressed as it is becoming a key enabling technology for the future growth of electronics. This work is motivated by the need to address this issue at the component (chip) level. The methodology presented here can be used for optimal design of on-chip microchannel heat sinks with

* Tel.: +1 804 8284267.
E-mail address: mmital@vcu.edu.

1359-4311/$ – see front matter © 2012 Elsevier Ltd. All rights reserved.
http://dx.doi.org/10.1016/j.applthermaleng.2012.07.040

nanofluid flow. The current study takes into consideration that the flow is not fully developed due to the short length of these microchannels (literature review reveals that often the optimization is done using fully developed heat transfer and pumping power correlations). Furthermore, the current study takes into consideration the increase in pumping power due to nanoparticle addition (whereas several studies in the literature perform this optimization by only considering the benefit of particle addition at a given flow rate, and not the pumping power penalty).

1.1. Micro-channel cooling for thermal management

Micro-channels are compact cooling elements that can provide increased heat dissipation rates and reduced temperature gradients across electronic components. Unlike traditional heat sinks that need a large surface area to increase heat dissipation rates, microchannels use small diameter channels to increase the heat transfer coefficient by forcing the coolant to flow in close contact with the channel walls. The heat transfer coefficient (and therefore, the heat dissipation) increases as the flow channel diameter is decreased. Based on channel diameter, Mehendale et al. [1] classified the range from 1 to 100 μm as microchannels, 100 μm to 1 mm as meso-channels, 1–6 mm as compact passages, and larger than 6 mm as traditional passages.

Several features of microchannel flow require careful evaluation. The continuum assumption and the applicability of Navier–Stokes equations to adequately model the flow and heat transfer behavior in microchannels need to be carefully evaluated for gas flows in small channels. For liquid flow, the distance between molecules is much smaller (on the order of angstroms) compared to the channel diameter (on the order of microns), which means the continuum assumption is still valid. Although some researchers have reported that compared to larger diameter passages, the flow transition (from laminar to turbulent) in micro-channels occurs at a much lower Reynolds number, recent studies by Bucci et al. [2] and Baviere et al. [3] have proved that the transitional Reynolds number of around 2300 is still valid for micro-channels.

Kandlikar and Grande [4] provide a review of the evolution of micro-channel technology, both in terms of their performance and the processes used to fabrication them. Tuckerman and Pease [5] were the first to propose the use of micro-channel cooling, and showed that heat transfer coefficients on the order of 10^5 W/m^2 K can be achieved, corresponding to cooling capabilities of up to 790 W/cm^2 using water as the coolant. Several researchers have studied the design and optimization of micro-channel cooled systems to achieve maximum cooling efficiency in electronic components. Lee [6] presented the design and optimization of an IGBT power electronic module by utilizing CFD techniques, and Bau [7] computed the thermal resistance of a flat plate micro heat exchanger with uniformly heated surfaces. Bau showed that the maximum temperatures can be minimized using non-uniform cross section conduits where the width varies as a function of the axial coordinate. Chen et al. [8] conducted numerical and experimental analyses to determine the maximum power that can be dissipated using single-phase liquid cooling on a stacked multi-chip module, if temperatures are to be maintained within reasonable limits. The stacked module consisted of three chips mounted on top of one another and separated by carriers. The parameters in this study included the input power, flow rate and coolants.

The studies in literature demonstrate that although micro-channel technology initially suffered from disadvantages such as high manufacturing, maintenance and sealing costs, large pressure drops in the channels, and fouling of the liquid, recent advances in manufacturing processes and related technologies show prospects of successfully overcoming these challenges.

1.2. Microchannel cooling using nanofluids

The removal of heat using microchannel heat sinks can be enhanced using nanofluids (liquid solutions with dispersed nanometer-sized particles) as reported by numerous studies literature [9–43]. This enhancement has been attributed to changes in effective thermophysical properties (increase in thermal conductivity and decrease in viscosity), although the exact mechanisms are currently not well-understood and are an area of active research. Several researchers have investigated the reason for enhanced heat transfer in nanofluids. Das et al. [44] have noted that the properties of a nanofluid (especially thermal conductivity and viscosity) cannot be estimated as weighted average of the fluid and solid nanoparticle components using simple mixture rules. This is because the properties of a nanofluid depend of several factors (related to nanofluid microstructure) such as the component properties, component volume fractions, particle size, particle geometry, particle distribution, matrix–particle interfacial effects, and particle motion. The particle motion (believed to have a significant contribution to enhanced heat transfer observed in nanofluids) is governed by superposition of several effects (thermophoresis, Saffman lift force, Brownian motion, Soret and Dufour effects, etcetera), some of which are not yet fully understood since they only become significant at very small length scales. Wang et al. [45] reported that a combination of several factors such as particle motion, surface action, and electro-kinetic effects caused the enhanced heat transfer in nanofluids. This study was the first to suggest that particle size may be an important contributing factor. Xuan and Li [46] suggested increased surface area of particles per unit volume, collision between particles, and the dispersion of particles as the reason for enhanced heat transport. The reasons proposed by Keblinski et al. [47] include Brownian motion of the particles, molecular-level layering of the liquid at the liquid/particle interface, the nature of heat transport in the nanoparticles, and the effects of nanoparticle clustering. They reported that the key factors are ballistic rather than diffusive nature of heat transport in the nanoparticles, combined with clustering effects that provide paths for rapid heat transport. Buongiorno [48] considered seven possible fluid–particle interaction effects in nanofluid convection (diffusion, inertia, thermophoresis, diffusionphoresis, Magnus effect, fluid drainage, and gravity). He concluded that Brownian diffusion and thermophoresis play an important role in laminar flow and turbulent viscous layer, but are insignificant in the turbulent region, where eddies dominate the motion of nanoparticles.

It is extremely difficult to theoretically estimate the thermophysical properties of nanofluids (since the details of the microstructure and the small scale effects are usually not known accurately), which makes the numerical modeling the nanoparticle flow challenging. Two approaches for dealing with this challenge are summarized below.

1.3. Modeling nanofluids

A first potential approach to modeling nanofluids uses discrete phase modeling (DPM) and is referred to as the Euler–Lagrangian method. The fluid is treated as a continuous media and the flow field is solved based on Navier–Stokes equations. The nanoparticles are individually tracked in a Lagrangian reference frame. The motion of each nanoparticle is determined using force balance and taking into account all local forces on the particle (gravity, thermophoretic, Saffman lift, drag, Brownian, Soret and Dufour, etcetera). The nanoparticles can exchange momentum, mass, and energy with the Euler frame fluid phase, and vice versa (if two way coupling is specified). The DPM approach can be computationally very time consuming, especially if there are a large number of particles.

Therefore, the current work uses another modeling approach (called the single phase approach) that implements experimental data to find empirical thermophysical property correlations (usually polynomials) that best fit the data. The particles and the base fluid mixture are treated as a single fluid with enhanced thermophysical properties, where the enhanced thermophysical properties are evaluated using experimental correlations rather than simple binary mixture rules. However, experimental data in the current literature is scarce, and reliable empirical correlations are only available for thermal conductivity and viscosity of nanofluids. Several researchers [49–51] have compared the accuracy of the two modeling approaches and reported comparable results.

2. Modeling

2.1. Model geometry and problem description

An integrated circuit (IC) chip is shown in Fig. 1. The electronic chip has a length L and width W of 10 mm, and a thickness H of 0.5 mm. Nanofluid coolant flows through parallel circular passages with diameter D of 0.1 mm. A constant axial inlet velocity V_0 and a constant temperature T_0 of 300 K are applied at the inlet of the circular channel. No-slip flow condition and a constant heat flux are imposed on the channel wall. The flow is assumed to be steady and incompressible. Assuming that the heat generation inside the chip is volumetric and uniform, a uniform heat flux q'' of 150 W/cm^2 is assumed at the channel walls. Rahman et al. [52] recently presented heat transfer analysis of a magnetic micro-cooler for NASA applications, where circular microchannels are embedded in rectangular solid substrate with volumetric heat generation (due to an imposed magnetic field). Due to the symmetry of the problem, only a unit cell consisting of a single channel needs to be considered as the computational domain.

In cases where the heat generation in the chip is non-uniform (such as when the heat generation is at the bottom surface of the chip), the channel walls will be subjected to a non-uniform circumferential and axial heat flux. For such cases, evaluating the heat transfer capabilities and optimization of the heat sink will require use of a 3D finite element or finite volume software package. Since 3D optimization studies are computationally expensive and time consuming, the current numerical model can be used to obtain an approximate solution (initial guess) for further detailed evaluations. The current model is also used to study the relative importance of the parameters (Reynolds number, nanoparticle size and particle volume fraction) on the thermal performance of the nanofluid heat sink.

2.2. Thermophysical properties

The thermophysical properties used in this study are based on the correlations from literature described below. In the absence of available data in the literature, the effective density and specific heat of the nanofluid (nf) are taken as the average of fluid and solid particle densities (based on the volume fraction ϕ of the particles in the suspension).

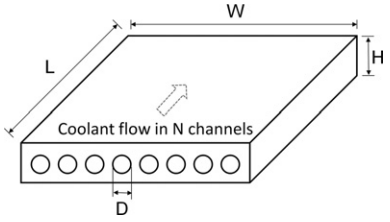

Fig. 1. The IC heat sink.

Table 1
Thermophysical properties used in the numerical model [55].

	Water	Alumina
Density (kg/m^3)	996.54	3989.22
Specific heat (J/kg K)	4177.78	778.92
Thermal conductivity (W/m K)	0.61	34.63
Viscosity (kg/s)	0.000866	–

$$\rho_{nf} = (1-\phi)\rho_{bf} + \phi\rho_p \tag{1}$$

$$c_{nf} = (1-\phi)c_{bf} + \phi c_p \tag{2}$$

The effective thermal conductivity is calculated using the model proposed by Chon et al. [53]:

$$\frac{k_{nf}}{k_{bf}} = 1 + 64.7\phi^{0.7460}\left(\frac{d_{bf}}{d_p}\right)^{0.3690}\left(\frac{k_p}{k_{bf}}\right)^{0.7476} Pr^{0.9955}Re^{1.2321} \tag{3}$$

The Prandtl number Pr, and the Reynolds number Re in Equation (3) are defined as:

$$Pr = \frac{\mu_{bf}}{\rho_{bf}\alpha_{bf}} \tag{4}$$

$$Re = \frac{\rho_{bf}BT}{3\pi\mu_{bf}^2 l_{bf}} \tag{5}$$

where the subscript bf denotes a property of base fluid (water), B is the Boltzmann constant (1.3807×10^{-23} J/K), and l_{bf} is the mean free path of base fluid molecules (0.17 nm for water molecules).

Maiga et al. [54] proposed a model for viscosity of dilute fluids with spherical nanoparticles, given by

$$\mu_{nf} = \mu_{bf}\left(1 + 7.3\phi + 123\phi^2\right) \tag{6}$$

The properties of water and alumina (evaluated at 300 K) used in Equations (1)–(6) are taken from Touloukian [55] and summarized in Table 1.

2.3. Correlations for modeling heat transfer and pumping power

Churchill and Ozoe [56] proposed the following correlation for local Nusselt number in the channel (assuming hydrodynamically and thermally developing flow conditions):

$$\frac{Nu_x}{4.364\left[1+\left(\frac{Gz}{29.6}\right)^2\right]^{1/6}} = \left\{1 + \frac{Gz/19.04}{\left[1+\left(\frac{Pr}{0.0207}\right)^{2/3}\left(1+\left(\frac{Gz}{29.6}\right)^2\right)^{1/3}\right]^{2/3}}\right\}^{1/3} \tag{7}$$

Here, Gz is the Graetz number given as:

$$Gz = \frac{\pi D Re_D Pr}{4x} \tag{8}$$

Equation (7) can be used for estimating the local Nusselt number at any given position along the length of the channel,

which can then be used to calculate the local heat transfer coefficient as:

$$h_x = \frac{k_{nf} Nu_x}{D} \tag{9}$$

The average heat transfer coefficient h_{av} is obtained by integrating the local heat transfer coefficient (Equation (9)) over the length L of the channel:

$$h_{av} = \frac{1}{L}\int_0^L h_x dx \tag{10}$$

Equation (10) is proposed to calculate the average heat transfer coefficient since the typical microchannel passage length L in electronics chips is much shorter than the entry length needed to achieve a fully developed flow. Using existing correlations from literature for average heat transfer coefficient in fully developed flow will yield significantly lower values.

After obtaining the average heat transfer coefficient, we also need to evaluate the pumping power needed to move the nanofluid through the channel. By considering the force balance between the pressure that drives the flow and the opposing friction force due to wall shear stress, we can write an expression for pressure drop dp over a segment dx of a single channel as:

$$dp = \frac{2 \times Po \times \mu \times V_m \times dx}{D^2} \tag{11}$$

where Po is called the Poiseuille number, V_m is the mean velocity, and μ is the dynamic viscosity of the nanofluid coolant. The Poiseuille number is a product of fanning friction factor f and flow Reynolds number, Re. The fanning friction factor is one-fourth of the Darcy friction factor. The Poiseuille number in developing flow varies along the length of the channel and is given as [57]:

$$f_{app}Re = \frac{3.44}{\sqrt{x^+}} + \frac{(fRe) + K_\infty/(4x^+) - 3.44/\sqrt{x^+}}{1 + C/(x^+)^2} \tag{12}$$

$$x^+ = \frac{x}{Re_D D} \tag{13}$$

where $f \times Re$ and K_∞ are constants for hydrodynamically developed flow. The values of $f \times Re$ and K_∞ (16 and 1.25) are adopted from Shah [57]. The total pressure drop Δp over the entire length of a single channel is obtained by substituting Equation (12) into Equation (11), and then integrating over the length L of the channel. The pumping power required to drive the fluid through the channel of the heat sink is the product of pressure drop and flow rate:

$$\overline{P} = \Delta p \times \pi \times \left(D^2/4\right) \times V_m \tag{14}$$

In order to evaluate the benefit of nanoparticle addition, the phrase heat transfer enhancement ratio (HTR) is defined as the ratio between the average heat transfer coefficient with the solid–liquid nanoparticle mixture and the heat transfer coefficient with the liquid phase only, at specified constant pumping power.

$$\mathrm{HTR} = \frac{h_{nf}}{h_{bf}} = f(d_p, Re, \phi) \tag{15}$$

Using our numerical model and statistical analysis, the HTR is evaluated as a function of particle diameter d_p, Reynolds number Re, and particle volume fraction ϕ.

2.4. Model validation

In order to validate the numerical model, the simulation results are compared with the experimental data from literature. Kim et al. [58] performed an experimental study to investigate the effects of nanofluids on convective heat transfer in a straight circular tube ($D = 4.57$ mm, $L = 2$ m) subjected to uniform heat flux of 2090 W/m^2 on the tube wall. A 3 percent alumina–water nanofluid at 22 °C was used as the coolant. The average size of the alumina nanoparticle was 35 nm. The heat transfer coefficient was measured as a function Reynolds number.

Anoop et al. [59] experimentally investigated convective heat transfer for developing laminar flow using alumina particles with size of 45 nm and 150 nm. A copper tube of 1.2 m length and 4.75 mm inner diameter was uniformly heated with power input of 200 W. The heat transfer coefficient was measured as a function of Reynolds number.

The model sensitivity and uncertainty analysis presented by Beck and Arnold [60] are used to account for the differences between the model presented here and the experimental data. The uncertainty in the current model arises because the model input parameters (such as particle diameter and volume fraction) are only estimates for the unknown actual values present during the physical experiments. Furthermore, the semi-empirical correlations for nanofluid thermophysical properties are a source of uncertainty since they are approximations for the unknown true relationships. The first step in sensitivity and uncertainty analysis is to identify the critical input parameters. Then, for output parameter $\eta(\boldsymbol{\beta})$ that depends on the input parameters $\boldsymbol{\beta}$, the first order derivative of $\eta(\boldsymbol{\beta})$ with respect to β_i is called the sensitivity coefficient for β_i. Sensitivity coefficients are important since they indicate the magnitude of the change in response η due to perturbations in the values of input parameters. These sensitivity coefficients can be written in dimensionless form given by:

$$X_i^+ = \frac{\partial \eta/\eta_0}{\partial \beta_i/\beta_{i0}} \tag{16}$$

where η_0 and β_{i0} are nominal values of output and input parameters (at the nominal experimental operating conditions) respectively. In the present study, the input parameters are the Reynolds number, applied heat flux, effective thermophysical properties (density, specific heat, thermal conductivity and viscosity) of the nanofluid, particle volume fraction and particle diameter. The output parameters are the values of local heat transfer coefficients, and the average heat transfer coefficient. Using Equation (16), the dimensionless predictive uncertainty associated with each input parameter can be calculated as:

$$\sigma_i^+ = X_i^+ \left(\frac{\sigma_M}{\beta_i}\right) \tag{17}$$

where the term in the brackets represents the measurement uncertainty. A measurement uncertainty of ±5% is used to suggest the upper and lower bounds about the nominal value of the input parameters, within which the actual value of the parameter is most likely to occur. The overall dimensionless uncertainty (ODU) can be calculated as the root-mean-square average of the uncertainty contributed by all the N input parameters:

$$\sigma^+ = \sqrt{\sum_{i=1}^{N}\left(\sigma_i^+\right)^2} \tag{18}$$

Using Equation (18), an ODU can be calculated in the prediction of a local heat transfer coefficient, and also in the prediction of average

heat transfer coefficient. An error bound ($\pm W/m^2$ K) can be associated with any predicted value by multiplying that value with its ODU.

3. Results and discussions

The results of model validation are presented in Figs. 2 and 3. In Fig. 2, our model over-predicts the experimental value of local heat transfer coefficient by a relative error of 15 percent near the channel entrance. In Fig. 3, it can be seen that at all Reynolds numbers, the average heat transfer coefficient predicted by our model is in good agreement with the experimental value.

The validated model and statistical analysis [61] are used to evaluate HTR (introduced in Equation (15)) as a function of design variables. The first step in statistical analysis is to get a response surface that approximates the relationship between the response HTR and the set of scaled input design variables as shown below:

$$\mathrm{HTR} = f\left(d^*, Re^*, \phi^*\right) \tag{19}$$

This response surface is estimated using a second-order polynomial with transformational and interaction terms as given below:

$$\mathrm{HTR} = \beta_0 + \sum_{i=1}^{N}\beta_i X_i + \sum_{i=1}^{N}\beta_{ii}X_i^2 + \sum_{i=1}^{N}\sum_{j=1}^{N}\beta_{ij}X_iX_j + \varepsilon \quad i,j = 1,2,3\ldots \tag{20}$$

In the above model Equations (20), X_1, X_2, … X_N are the N predictors of the response, β_0 is the intercept term and β_i are the regression coefficients. The response function is a quadratic function of X_1, X_2, … X_N. The product term X_iX_j represents the interaction of X_i and X_j. The coefficient β_{ij} therefore represents the effect of the interaction of X_i and X_j on HTR. The ε is the random error which is assumed to have a Gaussian distribution and expected value $E(\varepsilon)$ equal to zero. The method of least squares was used to obtain a good fit by minimizing the sum of squared residuals. A lower sum of the squared residual corresponds to a better match between the actual model and the polynomial that approximates the model.

Table 2 shows the linear regression model for heat transfer coefficient enhancement as a function of the input variables. Linear models (that is, linear in parameters) were found to be adequate ($R^2 > 0.95$) for representing the heat transfer coefficient enhancement. The regression model is valid for particle diameter d_p between 10 and 50 nm, Reynolds number between 250 and 1250, and volume fraction ϕ is between 1 and 7 percent. These variable ranges are determined after considering the valid ranges of the empirical thermophysical property correlations used in this study. All inputs are scaled between 0 and 1 using the upper limit of their respective range. This is done for regression analysis, and to make the magnitude of the resulting regression coefficients more meaningful and comparable. A '*' superscript is used to denote scaled (non-dimensional) inputs. Table 2 shows that volume fraction is the most significant factor impacting the value of HTR, followed by the particle diameter. The impact of the Reynolds number and other interaction terms is relatively weak.

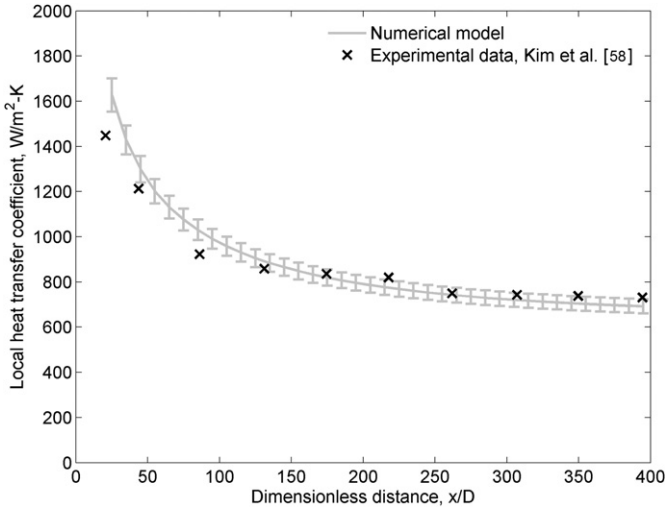

Fig. 2. Local heat transfer coefficient versus axial distance from numerical model and experiments.

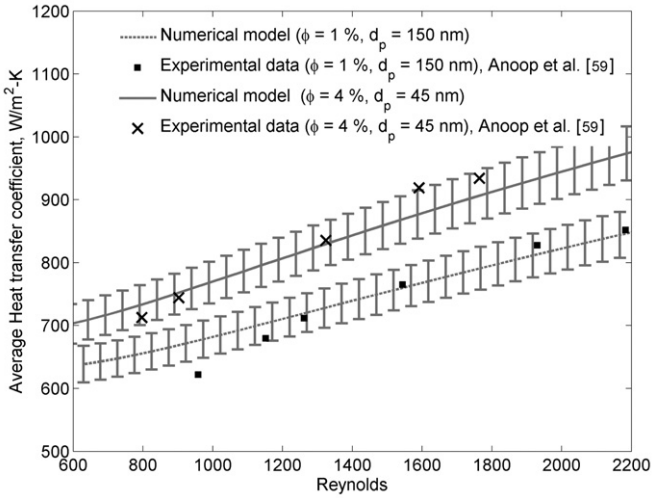

Fig. 3. Average heat transfer coefficient versus Reynolds number from numerical model and experiments.

The root mean square (RMS), R^2 and adjusted R^2 values are measures of how well the polynomial approximates the model. The RMS term represents the standard distance data values fall from the regression model curve. The low RMS value of 0.0042 means that the regression polynomial is reasonably accurate. The R^2 value of 0.9515 indicates that changes in the Reynolds number, particle diameter and particle volume fraction explain 95.15 percent of variation in the response. The R^2 (0.9515) and adjusted R^2 (0.9509) are virtually the same, indicating that our polynomial does not contain any unnecessary predictor terms.

Table 2
Regression analysis for heat transfer coefficient enhancement.

R-Square	95.150 percent
R-Square adjusted	95.090 percent
Root mean square error	0.004
Mean of response	1.041
Observations	729

	Estimate	Std error	*t* Ratio	*p*-Value
Constant	1.056	0.002	545.675	0.000
d^*	−0.113	0.004	−30.113	0.000
Re^*	−0.036	0.004	−9.617	0.000
ϕ^*	0.170	0.003	52.139	0.000
$(d^*)^2$	0.074	0.003	28.013	0.000
$(Re^*)^2$	0.024	0.003	8.971	0.000
$(\phi^*)^2$	−0.081	0.002	−34.917	0.000
$(d^*)(Re^*)$	0.011	0.002	4.686	0.000
$(Re^*)(\phi^*)$	−0.036	0.002	−16.774	0.000
$(d^*)(\phi^*)$	−0.068	0.002	−31.526	0.000

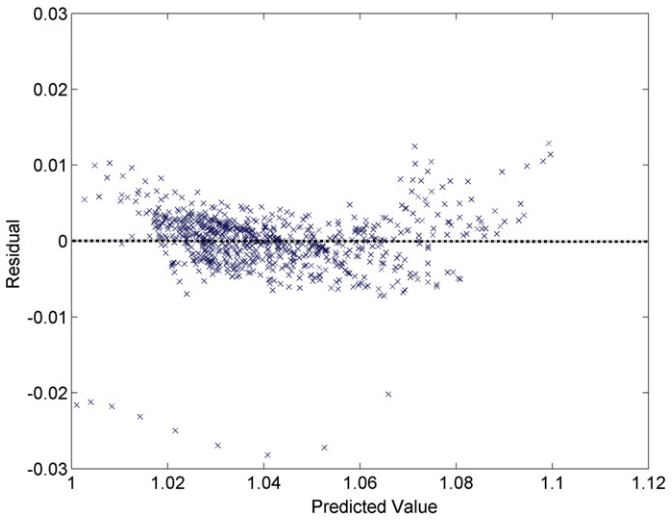

Fig. 4. Residual plot of the heat transfer enhancement regression model.

In order for the polynomial fit to be valid despite a good R^2 value, the residual plot of the response must be analyzed. There should be no correlation in data points in a satisfactory residual plot. The residual plot of HTR (Fig. 4) shows that the points are distributed evenly around the zero line without showing any form of correlation or pattern. This satisfies the assumption of constant variance. If the data points were not evenly distributed around the mean, then transformational terms would have to be added to the polynomial equation to accommodate for the correlation present in the data in residual plot.

In general the average heat transfer in developing flow improves with smaller diameter particles, higher volume fraction of the particles, and higher Reynolds number. However, the improvement is partially offset due to additional pumping power penalty. The pumping power penalty is often neglected in literature, and the heat transfer improvement of nanofluids over base fluid is reported at a specified Reynolds number or flow rate. In order to evaluate the gain of nanoparticle addition, the heat transfer using nanofluid must be compared with heat transfer using base fluid at a fixed operating cost (pumping power). The parameter HTR introduced in Equation (15) is used to quantify this gain as a function of the inputs. Fig. 5 shows the variation of HTR with volume fraction, considering high and low levels (250 and 1250 respectively) of Reynolds number and two levels (10 and 50 nm) of particle size. The figure shows that HTR is higher for smaller particle diameter, which is expected since smaller particle size improves heat transfer but does not contribute to an increase in pumping power (the experimental data and correlations show that the nanofluid viscosity depends very weakly on particle size). Currently no experimental data are available for behavior of particles smaller than 10 nm, so it can be used as lower limit on the particle size until more data becomes available. Fig. 5 also shows that HTR is higher for lower Reynolds number, which means that the benefit of adding the nanoparticles is more pronounced at lower flow rates. Finally, HTR shows parabolic variation with volume fraction. After determining the Reynolds number (based on available pumping power), and the smallest available particle diameter, there exists an optimum value of volume fraction that would maximize HTR value. Not taking the pumping power into consideration would have led to the absurd conclusion that the performance would improve indefinitely with higher volume fraction.

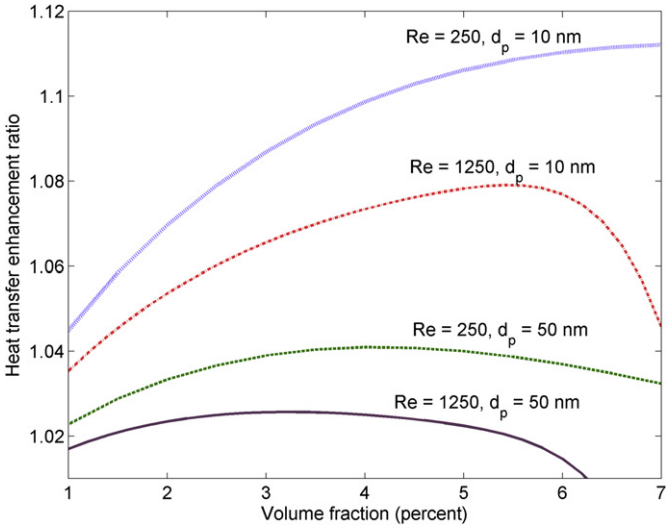

Fig. 5. Average heat transfer coefficient enhancement versus volume fraction for different Reynolds numbers.

4. Conclusions

A semi-empirical numerical model is presented to evaluate the heat transfer and flow characteristics of nanofluid microchannel heat sink with laminar forced convection. The model is flexible enough to be extended to the case of non-uniform heat flux on the channel walls in future studies. It can be used to predict the tradeoff between heat transfer improvement and increased pumping power due to the addition of nanoparticles in the base fluid. The phrase heat transfer enhancement ratio (HTR) is used to denote the ratio of average heat transfer coefficient of nanofluid to water at the same pumping power. The validated model is used to study the impact of design variables (Reynolds number, volume fraction and particle size) on the HTR. Statistical analysis of the model showed that the volume fraction is the most significant factor impacting the HTR, followed by the particle diameter. The impact of the Reynolds number and other interaction terms is relatively weak. The HTR is maximized at smallest possible particle diameter (since smaller particles improve heat transfer but do not impact pumping power). HTR is higher for lower Reynolds number, which means that the benefit of adding the nanoparticles is more pronounced at lower flow rates. The HTR shows parabolic variation with volume fraction. After determining the Reynolds number (based on available pumping power), and the smallest available particle diameter, there exists an optimum value of volume fraction that would maximize HTR value. The methodology and results presented here would be useful for understanding and optimal design of microchannel heat sinks with nanofluid flow.

Nomenclature

c	specific heat
dx	differential length along the channel wall (m)
d	diameter (m)
D	channel diameter (m)
f	fanning friction factor
Gz	Graetz number
h	heat transfer coefficient (W/m^2 K)
H	height (meter)
k	thermal conductivity (W/m K)
l, L	length (m)
Nu	Nusselt number

p	pressure (N/m^2)
$\overline{P}$	pumping power (W)
Po	Poiseuille number
Pr	Prandtl number
q	heat transfer (W)
R	thermal resistance
Re	Reynolds number
T	temperature, °C
V	velocity (m/s)
W	width (m)
x	axial distance (m)
X	sensitivity coefficient

Greek symbols

α	thermal diffusivity (m^2/s)
$\boldsymbol{\beta}$	model input parameters vector
β	model input parameter
ρ	density (kg/m^3)
∇	gradient operator
μ	viscosity (kg/m s)
η	model output
ϕ	percent volume fraction
ν	kinematic viscosity (m^2/s)
Ω	heat transfer of nanofluid over heat transfer of base fluid at same pumping power

Subscripts

0	reference or inlet value
av	average
bf	base fluid (water)
D	property evaluated based on diameter or hydraulic diameter
i	ith parameter or variable
nf	nanofluid (Al_2O_3–water)
m	mean/average
p	nanoparticle

Superscripts

+	dimensionless quantity

References

[1] S.S. Mehendale, A.M. Jacobi, R.K. Shah, Fluid flow and heat transfer at micro- and meso-scales with applications to heat exchanger design, Applied Mechanics Review 53 (7) (2000) 175–193.

[2] A. Bucci, G.P. Celata, M. Cumo, E. Serra, G. Zummo, Water single-phase fluid flow and heat transfer in capillary tubes, in: Proceedings of First International Conference on Microchannels and Minichannels, American Society of Mechanical Engineers, Rochester, New York, 2004, pp. 319–326.

[3] R. Baviere, F. Ayela, S.L. Person, M. Favre-Marinet, An experimental study of water flow in smooth and rough rectangular micro-channels, in: Second International Conference on Microchannels and Minichannels, American Society of Mechanical Engineers, Rochester, New York, 2004, pp. 221–228.

[4] S.G. Kandlikar, W.J. Grande, Evolution of microchannel flow passages – thermohydraulic performance and fabrication technology, Heat Transfer Engineering 24 (1) (2003) 3–17.

[5] D.B. Tuckerman, R.F. Pease, High performance heat sinking for VLSI, IEEE Electronic Device Letters 2 (5) (1981) 126–129.

[6] T. Lee, Design optimization of an integrated liquid-cooled IGBT power module using CFD technique, IEEE Transactions on Components and Packaging Technologies 23 (1) (2000) 55–60.

[7] H.H. Bau, Optimization of conduits shape in micro heat exchangers, International Journal of Heat and Mass Transfer 41 (1998) 2717–2723.

[8] X.Y. Chen, K.C. Toh, T.N. Wong, J.C. Chai, Direct liquid cooling of stacked MCM, in: Proceedings of Ninth Inter-society Conference on Thermal and Thermomechanical Phenomena in Electronic Systems, Institute of Electrical and Electronics Engineers, Las Vegas, Nevada, 2004, pp. 199–206.

[9] H.R. Seyf, B. Nikaaein, Analysis of Brownian motion and particle size effects on the thermal behavior and cooling performance of microchannel heat sinks, International Journal of Thermal Sciences 58 (2012) 36–44.

[10] M. Kalteh, A. Abbassi, M. Saffar-Avval, A. Frijns, A. Darhuber, J. Harting, Experimental and numerical investigation of nanofluid forced convection inside a wide microchannel heat sink, Applied Thermal Engineering 36 (1) (2012) 260–268.

[11] T.C. Hung, W.M. Yan, X.D. Wang, C.Y. Chang, Heat transfer enhancement in microchannel heat sinks using nanofluids, International Journal of Heat and Mass Transfer 55 (9–10) (2012) 2559–2570.

[12] M.D. Byrne, R.A. Hart, A.K. Da Silva, Experimental thermal–hydraulic evaluation of CuO nanofluids in microchannels at various concentrations with and without suspension enhancers, International Journal of Heat and Mass Transfer 55 (9–10) (2012) 2684–2691.

[13] S.M. Aminossadati, A. Raisi, B. Ghasemi, Effects of magnetic field on nanofluid forced convection in a partially heated microchannel, International Journal of Non-Linear Mechanics 46 (10) (2011) 1373–1382.

[14] Y.T. Yang, F.H. Lai, Lattice Boltzmann simulation of heat transfer and fluid flow in a microchannel with nanofluids, Heat and Mass Transfer/Waerme- und Stoffuebertragung 47 (10) (2011) 1229–1240.

[15] D. Lelea, The performance evaluation of Al_2O_3/water nanofluid flow and heat transfer in microchannel heat sink, International Journal of Heat and Mass Transfer 54 (17–18) (2011) 3891–3899.

[16] H.A. Mohammed, P. Gunnasegaran, N.H. Shuaib, The impact of various nanofluid types on triangular microchannels heat sink cooling performance, International Communications in Heat and Mass Transfer 38 (6) (2011) 767–773.

[17] D. Lelea, C. Nisulescu, The micro-tube heat transfer and fluid flow of water based Al_2O_3 nanofluid with viscous dissipation, International Communications in Heat and Mass Transfer 38 (6) (2011) 704–710.

[18] A. Ramiar, A.A. Ranjbar, Effects of viscous dissipation and variable properties on nanofluids flow in two dimensional microchannels, International Journal of Engineering, Transactions A: Basics 24 (2) (2011) 131–142.

[19] Y.T. Yang, F.H. Lai, Numerical study of flow and heat transfer characteristics of alumina–water nanofluids in a microchannel using the lattice Boltzmann method, International Communications in Heat and Mass Transfer 38 (5) (2011) 607–614.

[20] H. Aminfar, R. Maroofiazar, A numerical study of the hydro-thermal behaviour of nanofluids in rectangular microchannels using a mixture model, Proceedings of the Institution of Mechanical Engineers, Part C: Journal of Mechanical Engineering Science 225 (4) (2011) 791–798.

[21] H.A. Mohammed, G. Bhaskaran, N.H. Shuaib, R. Saidur, Heat transfer and fluid flow characteristics in microchannels heat exchanger using nanofluids: a review, Renewable and Sustainable Energy Reviews 15 (3) (2011) 1502–1512.

[22] C.H. Chen, C.Y. Ding, Study on the thermal behavior and cooling performance of a nanofluid-cooled microchannel heat sink, International Journal of Thermal Sciences 50 (3) (2011) 378–384.

[23] A. Akbarinia, M. Abdolzadeh, R. Laur, Critical investigation of heat transfer enhancement using nanofluids in microchannels with slip and non-slip flow regimes, Applied Thermal Engineering 31 (4) (2011) 556–565.

[24] M. Kalteh, A. Abbassi, M. Saffar-Avval, J. Harting, Eulerian–Eulerian two-phase numerical simulation of nanofluid laminar forced convection in a microchannel, International Journal of Heat and Fluid Flow 32 (1) (2011) 107–116.

[25] H.A. Mohammed, P. Gunnasegaran, N.H. Shuaib, Influence of various base nanofluids and substrate materials on heat transfer in trapezoidal microchannel heat sinks, International Communications in Heat and Mass Transfer 38 (2) (2011) 194–201.

[26] A. Raisi, B. Ghasemi, S.M. Aminossadati, A numerical study on the forced convection of laminar nanofluid in a microchannel with both slip and no-slip conditions, Numerical Heat Transfer, Part A: Applications 59 (2) (2011) 114–129.

[27] E. Farsad, S.P. Abbasi, M.S. Zabihi, J. Sabbaghzadeh, Numerical simulation of heat transfer in a micro channel heat sinks using nanofluids, Heat and Mass Transfer/Waerme- und Stoffuebertragung 47 (4) (2011) 479–490.

[28] J. Li, C. Kleinstreuer, Entropy generation analysis for nanofluid flow in microchannels, Journal of Heat Transfer 132 (12) (2010). art. no. 122401.

[29] H.A. Mohammed, P. Gunnasegaran, N.H. Shuaib, Heat transfer in rectangular microchannels heat sink using nanofluids, International Communications in Heat and Mass Transfer 37 (10) (2010) 1496–1503.

[30] R.H. Khiabani, Y. Joshi, C.K. Aidun, Heat transfer in microchannels with suspended solid particles: lattice-Boltzmann based computations, Journal of Heat Transfer 132 (4) (2010) 1–9.

[31] C.J. Ho, L.C. Wei, Z.W. Li, An experimental investigation of forced convective cooling performance of a microchannel heat sink with Al_2O_3/water nanofluid, Applied Thermal Engineering 30 (2–3) (2010) 96–103.

[32] C.T. Nguyen, M. Le Menn, Two-phase modelling of nanofluid heat transfer in a microchannel heat sink, WIT Transactions on Modeling and Simulation 48 (2009) 451–460.

[33] M. Ghazvini, M.A. Akhavan-Behabadi, M. Esmaeili, The effect of viscous dissipation on laminar nanofluid flow in a microchannel heat sink, Proceedings of the Institution of Mechanical Engineers, Part C: Journal of Mechanical Engineering Science 223 (11) (2009) 2697–2706.

[34] M. Ghazvini, H. Shokouhmand, Investigation of a nanofluid-cooled microchannel heat sink using fin and porous media approaches, Energy Conversion and Management 50 (9) (2009) 2373–2380.

[35] P. Bhattacharya, A.N. Samanta, S. Chakraborty, Numerical study of conjugate heat transfer in rectangular microchannel heat sink with Al_2O_3/H_2O nanofluid, Heat and Mass Transfer/Waerme- und Stoffuebertragung 45 (10) (2009) 1323–1333.

[36] J. Li, C. Kleinstreuer, Microfluidics analysis of nanoparticle mixing in a microchannel system, Microfluidics and Nanofluidics 6 (5) (2009) 661–668.
[37] P. Mehraban Rad, C. Aghanajafi, The effect of thermal radiation on nanofluid cooled microchannels, Journal of Fusion Energy 28 (1) (2009) 91–100.
[38] J.-Y. Jung, H.-S. Oh, H.-Y. Kwak, Forced convective heat transfer of nanofluids in microchannels, International Journal of Heat and Mass Transfer 52 (1–2) (2009) 466–472.
[39] J. Li, C. Kleinstreuer, Thermal performance of nanofluid flow in microchannels, International Journal of Heat and Fluid Flow 29 (4) (2008) 1221–1232.
[40] J. Chevalier, O. Tillement, F. Ayela, Rheological properties of nanofluids flowing through microchannels, Applied Physics Letters 91 (23) (2007). art. no. 233103.
[41] T.-H. Tsai, R. Chein, Performance analysis of nanofluid-cooled microchannel heat sinks, International Journal of Heat and Fluid Flow 28 (5) (2007) 1013–1026.
[42] J. Lee, I. Mudawar, Assessment of the effectiveness of nanofluids for single-phase and two-phase heat transfer in micro-channels, International Journal of Heat and Mass Transfer 50 (3–4) (2007) 452–463.
[43] R. Chein, J. Chuang, Experimental microchannel heat sink performance studies using nanofluids, International Journal of Thermal Sciences 46 (1) (2007) 57–66.
[44] S.K. Das, S.U. Choi, W. Yu, T. Pradeep, Nanofluids: Science and Technology, John Wiley & Sons, New Jersey, 2008.
[45] X. Wang, X. Xu, S.U.S. Choi, Thermal conductivity of nanoparticle–fluid mixture, Journal of Thermophysics and Heat Transfer 13 (4) (1999) 474–480.
[46] Y. Xuan, Q. Li, Investigation on convective heat transfer and flow features of nanofluids, Journal of Heat Transfer 125 (1) (2003) 151–155.
[47] P. Keblinski, S.R. Phillpot, S.U.S. Choi, J.A. Eastman, Mechanisms of heat flow in suspensions of nano-sized particles (nanofluids), International Journal of Heat and Mass Transfer 45 (2002) 855–863.
[48] J. Buongiorno, Convective transport in nanofluids, Journal of Heat Transfer 128 (3) (2006) 240–250.
[49] R. Lotfi, Y. Saboohi, A.M. Rashidi, Numerical study of forced convective heat transfer of nanofluids: comparison of different approaches, International Communications in Heat and Mass Transfer 37 (1) (2010) 74–78.
[50] V. Bianco, F. Chiacchio, O. Manca, S. Nardini, Numerical investigation of nanofluids forced convection in circular tubes, Applied Thermal Engineering 29 (2009) 3632–3642.
[51] V. Bianco, O. Manca, S. Nardini, Numerical investigation on nanofluids turbulent convection heat transfer inside a circular tube, International Journal of Thermal Sciences 50 (2011) 341–349.
[52] M.M. Rahman, A.A. Gari, S. Shevade, Heat transfer in circular microchannels during volumetric heating with magnetic field, Heat and Mass Transfer 44 (4) (2007) 463–472.
[53] C.H. Chon, K.D. Kihm, S.P. Lee, S.U.S. Choi, Empirical correlation finding the role of temperature and particle size for nanofluid (Al_2O_3) thermal conductivity enhancement, Applied Physics Letters 87 (15) (2005) 1531071–1531073.
[54] S.E.B. Maiga, S.J. Palm, C.T. Nguyen, G. Roy, N. Galanis, Heat transfer enhancement by using nanofluids in forced convection flows, International Journal of Heat and Fluid Flow 26 (4) (2005) 530–546.
[55] Y.S. Touloukian, Thermophysical Properties of Matter: the TPRC Data Series, a Comprehensive Compilation of Data, IFI/Plenum, New York, 1970.
[56] S.W. Churchill, H. Ozoe, Correlations for laminar forced convection with uniform heating in flow over a plate and in developing and fully developed flow in a tube, ASME Journal of Heat Transfer 95 (1973) 78–84.
[57] R.K. Shah, A correlation for laminar hydrodynamic entry length solutions for circular and noncircular ducts, Journal of Fluids Engineering 100 (4) (1978) 177–179.
[58] D. Kim, Y. Kwon, Y. Cho, C. Li, S. Cheong, Y. Hwang, J. Lee, D. Hong, S. Moon, Convective heat transfer characteristics of nanofluids under laminar and turbulent flow conditions, Current Applied Physics 9 (2) (2009) 119–123.
[59] K.B. Anoop, T. Sundararajan, S.K. Das, Effect of particle size on the convective heat transfer in nanofluid in the developing region, International Journal of Heat and Mass Transfer 52 (9–10) (2009) 2189–2195.
[60] J.V. Beck, K.J. Arnold, Parameter Estimation in Science and Engineering, John Wiley & Sons, New York, 1977.
[61] W. Mendenhall, T. Sincich, Statistics for Engineering and the Sciences, fifth ed. Prentice Hall, New Jersey, 2007.